Molecular Biology of the Cell
Vol. 13, 3706–3719, October 2002

Mad2 and BubR1 Function in a Single Checkpoint Pathway that Responds to a Loss of Tension

Katie B. Shannon,*†‡ Julie C. Canman,† and E. D. Salmon†

*SPIRE fellow †Department of Biology, University of North Carolina, Chapel Hill, North Carolina 27599-3280

Submitted March 7, 2002; Revised June 19, 2002; Accepted July 8, 2002
Monitoring Editor: Tim Stearns

The spindle checkpoint monitors microtubule attachment and tension at kinetochores to ensure proper chromosome segregation. Previously, PtK1 cells in hypothermic conditions (23°C) were shown to have a pronounced mitotic delay, despite having normal numbers of kinetochore microtubules. At 23°C, we found that PtK1 cells remained in metaphase for an average of 101 min, compared with 21 min for cells at 37°C. The metaphase delay at 23°C was abrogated by injection of Mad2 inhibitors, showing that Mad2 and the spindle checkpoint were responsible for the prolonged metaphase. Live cell imaging showed that kinetochore Mad2 became undetectable soon after chromosome congression. Measurements of the stretch between sister kinetochores at metaphase found a 24% decrease in tension at 23°C, and metaphase kinetochores at 23°C exhibited higher levels of 3F3/2, Bub1, and BubR1 compared with 37°C. Microinjection of anti-BubR1 antibody abolished the metaphase delay at 23°C, indicating that the higher kinetochore levels of BubR1 may contribute to the delay. Disrupting both Mad2 and BubR1 function induced anaphase with the same timing as single inhibitions, suggesting that these checkpoint genes function in the same pathway. We conclude that reduced tension at kinetochores with a full complement of kinetochore microtubules induces a checkpoint dependent metaphase delay associated with elevated amounts of kinetochore 3F3/2, Bub1, and BubR1 labeling.

INTRODUCTION

The correct segregation of chromosomes is crucial to prevent aneuploidy. The spindle checkpoint senses attachment of kinetochores to the plus ends of spindle microtubules and prevents anaphase onset until chromosomes are aligned and kinetochores are under tension at the metaphase plate. A single unattached kinetochore is sufficient to delay anaphase, as destruction of the last unattached kinetochore induces anaphase onset, demonstrating that the "wait anaphase" signal is generated at kinetochores (Rieder *et al.*, 1995).

Many proteins required for the checkpoint were originally identified by genetic screens in the budding yeast *Saccharomyces cerevisiae*. The genes Mad 1–3 (Li and Murray, 1991) and Bub 1 and 3 (Hoyt *et al.*, 1991) are required for mitotic arrest and viability in the presence of microtubule poisons. Homologues of Mad1 (Chen *et al.*, 1998), Mad2 (Chen *et al.*, 1996; Li and Benezra, 1996), Bub1 (Taylor and McKeon, 1997; Sharp-Baker and Chen, 2001), and Bub3 (Taylor *et al.*, 1998) have been found in higher organisms, and the localization of these proteins is high on unattached kinetochores and diminishes as kinetochores acquire microtubules and are under increasing tension. A mammalian protein kinase that has homology to both Mad3 and Bub1, named BubR1, also localizes to mitotic kinetochores (Chan *et al.*, 1999). Use of mutants in yeast and dominant negative proteins or antibodies in tissue cells have shown that inhibition of a single checkpoint protein inactivates the checkpoint (Amon, 1999), allowing for anaphase in the absence of microtubules. Experiments also revealed that the mitotic checkpoint is involved in normal mitotic progression, as inactivation of the checkpoint in early mitosis can lead to premature anaphase onset without an intervening metaphase (Gorbsky *et al.*, 1998; Canman *et al.*, 2000).

The mitotic checkpoint controls anaphase onset by inhibiting the anaphase promoting complex/cyclosome (APC/C), a ubiquitin ligase. At anaphase, activation of APC/C by Cdc20 ubiquitinates securin, which is then degraded by the 26S proteasome. Securin protealysis results in sister-chromatid separation (King *et al.*, 1996; Zachariae and Nasmyth, 1999). The APC/C inhibitory signal is generated at the kinetochore because a single unattached kinetochore can inhibit anaphase onset (Rieder *et al.*, 1995). How the inhibitory signal is generated and how the checkpoint monitors microtubule attachment and/or tension at the kinetochore are topics of much debate. Microtubule attachment induces the

Article published online ahead of print. Mol. Biol. Cell 10.1091/mbc.E02–03–0137. Article and publication date are at www.molbiolcell.org/cgi/doi/10.1091/mbc.E02–03–0137.

‡ Corresponding author. E-mail address: ktphd@email.unc.edu.

loss of checkpoint proteins at kinetochores, in particular, a substantial loss of Mad2 (Waters *et al.*, 1998; Hoffman *et al.*, 2001). Mad2 is able to bind Cdc20 and inhibit APC/C activation in vitro (Li *et al.*, 1997; Fang *et al.*, 1998), and Mad2 turns over quickly at unattached kinetochores, with a half-life of 24–28 s (Howell *et al.*, 2000). The cycling of Mad2 on and off kinetochores is thought to be crucial for generating a soluble APC/C inhibitor, and Mad2 depletion from attached kinetochores may signal anaphase onset (Gorbsky *et al.*, 1998; Waters *et al.*, 1998; Hoffman *et al.*, 2001).

However, the checkpoint is also responsive to tension, as tension applied to a misattached kinetochore using a microneedle induces anaphase (Li and Nicklas, 1995). A tension-sensitive phosphorylation at the kinetochore detected by the 3F3/2 antibody has been shown to become dephosphorylated in response to tension (Gorbsky and Ricketts, 1993; Nicklas *et al.*, 1995). Kinetochores exhibit a "memory" of their 3F3/2 phosphorylation state after lysis (Campbell *et al.*, 2000), reflecting a chemical change that takes place at kinetochores in response to tension. Taxol treatment of metaphase cells causes loss of tension without a loss of kinetochore microtubles and results in substantial increases in the phophorylation detected by the 3F3/2 antibody (Waters *et al.*, 1998). Elevated levels of the kinases Bub1 and BubR1 at kinetochores in HeLa cells have been found in response to loss of tension caused by low concentrations of vinblastine (Skoufias *et al.*, 2001), and Bub1 levels increase in response to taxol (Taylor *et al.*, 2001). Thus, kinetochore localization of these checkpoint components appears sensitive to tension, independent of microtubule attachment, although tension also stabilizes microtubule attachment (Nicklas *et al.*, 2001). BubR1 interacts with the kinetochore motor CENP-E (Chan *et al.*, 1999), suggesting that BubR1 may be involved in linking the checkpoint to forces generating tension at the kinetochore. Recent work has shown that BubR1, either alone or in a complex, can bind to Cdc20 and act as an inhibitor of APC/C activation in vitro (Sudakin *et al.*, 2001; Tang *et al.*, 2001; Fang, 2002).

The molecular composition of the BubR1 inhibitory complex is uncertain. Sudakin *et al.* (2001) describe the isolation of an APC/C inhibitory complex from HeLa cells they named MCC (mitotic checkpoint complex), which contains BubR1, Bub3, Cdc20, and Mad2. The inhibitory activity of this complex in vitro is over 3000-fold greater than Mad2 alone. Other labs have found that in checkpoint-arrested cells, Cdc20 forms two separate complexes containing either BubR1 or Mad2 but not both (Fang, 2002; Tang *et al.*, 2001). In vitro assays show that BubR1 alone is able to bind and inhibit Cdc20-APC at much lower concentrations than Mad2 alone (Fang, 2002; Tang *et al.*, 2001). Addition of Mad2, but not Bub3, stimulates the inhibition of APC/C by BubR1 in vitro (Tang *et al.*, 2001; Fang, 2002). Therefore, BubR1 and Mad2 may act synergistically or in a complex to prevent APC/C activation.

However, Skoufias *et al.* (2001) recently proposed that Mad2 and BubR1 act in two independent checkpoint pathways monitoring microtubule attachment and tension, respectively. Conditions that result in a loss of tension but not kinetochore microtubules initially cause an increase in BubR1, but not Mad2 levels at kinetochores (Waters *et al.*, 1998; Skoufias *et al.*, 2001). The checkpoint arrest caused by vinblastine was not overcome by microinjection of anti-Mad2 antibodies (Skoufias *et al.*, 2001), suggesting that the checkpoint arrest caused by tension is Mad2 independent. However, a taxol-induced arrest that produces loss of tension but not attachment does require Mad2 (Waters *et al.*, 1998).

Previous studies on PtK1 cells under hypothermic conditions (23–25°C) showed a mitotic delay (Rieder, 1981), despite the attachment of normal numbers of kinetochore microtubules (Cassimeris *et al.*, 1988). We were interested in determining if this mitotic delay at low temperatures was due to the mitotic checkpoint and if so, which checkpoint proteins were involved.

MATERIALS AND METHODS

Cell Culture

PtK1 cells (American Type Culture Collection, Rockville, MD) were grown on coverslips and maintained in Ham's F12 medium, pH 7.2 (Sigma Chemical Co., St. Louis, MO) supplemented with 10% FBS, 100 U/ml penicillin, 0.1 mg/ml streptomycin, and 0.25 μg/ml amphotericin B in a 37°C, 5% CO_2 incubator. HeLa cells were maintained in DMEM (Life Technologies, Rockville, MD) supplemented with 10% FBS, 100 U/ml penicillin, 0.1 mg/ml streptomycin, and 0.25 μg/ml amphotericin B. For microinjection or filming experiments, cells were incubated in dye-free L-15 medium, pH 7.2 (Sigma Chemical Co.), supplemented as described for Ham's F12.

Immunofluorescence

Cells were lysed in freshly prepared 0.5% Triton X-100 in PHEM buffer (60 mM Pipes, 25 mM HEPES, 10 mM EGTA, 4 mM $MgSO_4$, pH 6.9) at 23 or 37°C. When staining for the phosphoprotein recognized by the 3F3/2 antibody, 100 nM microcystin (Sigma Chemical Co.) was included in the lysis buffer. Cells were then fixed in freshly prepared 4% formaldehyde in PHEM buffer at 23 or 37°C for 20 min. Cells were then rinsed three times for 5 min in PBS with 0.05% Tween-20 (PBST) and blocked overnight at 4°C in PHEM with 5% donkey serum. Primary antibodies were diluted into PHEM with 5% donkey serum, and cells were incubated at room temperature for 1 h. After three 5-min PBST washes, secondary donkey anti-rabbit, anti-mouse, or anti-human antibodies (diluted 1:100 in PHEM with 5% donkey serum) were added for 45 min.

CREST-SH serum was a gift from Dr. B.R. Brinkley (Baylor College of Medicine, Houston, TX) and used at 1:600. Affinity-purified BubR1 antibodies (Chan *et al.*, 1998) were used at 1:500 dilution. The mAb to the 3F3/2 antigen was provided by Dr. Gary Gorbsky (University of Oklahoma Health Sciences Center, Oklahoma City) and used at 1:5000 dilution. Antibodies to Mad2 were affinity purified as described (Waters *et al.*, 1998) and used at 1:50. Bub1 was detected using rabbit sera provided by Dr. Don Cleveland (University of California at San Diego) at 1:200.

Microinjection

Before microinjection, coverslips were mounted in modified Rose chambers (Rieder and Hard, 1990) lacking the top coverslip, and chambers were filled with L-15 media. A circle was inscribed on the bottom coverslip using a diamond-tip scribing objective (Carl Zeiss, Inc., Thornwood, NY) and was used as a reference to relocate injected cells. Injections were performed on a Zeiss IM microscope equipped with phase optics and a 40×/0.75 NA objective. The microinjection system is essentially as described (Waters *et al.*, 1996). For injection of anti-Mad2 antibody, antibody was affinity purified as previously described (Waters *et al.*, 1998) and injected at a needle concentration of 1–2 mg/ml. GST-Mad1F10 was purified as described (Canman *et al.*, 2002b) and injected at a needle concentration of 5 mg/ml in HEK (20 mM HEPES, 100 mM KCl, 1 mM DTT, pH

7.7). BubR1 antibody for injection was a gift from Dr. Guowei Fang (Stanford University, Stanford, CA) and was used at a needle concentration of 2.5 mg/ml in PBS (140 mM NaCl, 2.5 mM KCl, 10 mM Na_2HPO_4, and 1.5 mM KH_2PO_4, pH 7.8). For microinjection controls, rabbit IgG immunoglobulin at 5 mg/ml in injection buffer and GST at 5 mg/ml in HEK were used. The top of the chamber was sealed using mineral oil. Alexa488-XMad2 was prepared as described (Howell *et al.*, 2000), diluted into injection buffer (10 mM Na_2HPO_4, 100 mM KCl, 1 mM $MgCl_2$, pH 7.4), and injected at 2–3.5 μM needle concentration. These chambers were sealed using a top coverslip and filled using a syringe and needle with fresh, dye-free high-glucose L-15 medium supplemented with 0.3 U/ml the oxygen-scavenging enzyme Oxyrase (Oxyrase, Inc., Mansfield, OH).

Microscopy and Image Acquisition

Immunofluorescently labeled cells were viewed with a multimode digital fluorescence microscope system (Salmon *et al.*, 1994). Images were obtained with a Hamamatsu C4880 cooled CCD digital camera (Bridgewater, NJ), using a Nikon Microphot FX-A microscope (Garden City, NJ) equipped with a 60×/1.4 NA Phase 3 objective lens. Both phase contrast and fluorescence images were obtained for control and experimental cells. Digital images were acquired by MetaMorph image processing software (Universal Imaging Corp., West Chester, PA). Z-series optical sections through each cell were obtained at 0.5-μm steps, using MetaMorph software and a Ludl (Hawthorne, NY) stepping motor.

For live cell fluorescence and photobleaching studies, cells in modified Rose chambers with high-glucose L-15 with Oxyrase (as described above) were imaged on a Nikon TE300 inverted microscope equipped with a sensitive, Orca1-cooled CCD camera (Hamamatsu Photonics). Pairs of fluorescent and phase images were obtained using a 100× 1.4 NA Plan Apo Phase 3 objective, a 100-W mercury arc lamp light source, a 100-W Quartz-Halogen transilluminator, and a Chroma Hy-Q FITC filter set (Brattleboro, VT). Photobleaching experiments were performed as described (Howell *et al.*, 2000; Maddox *et al.*, 2000). In brief, a 488-nm line from an argon laser (Spectra Physics, Mountain View, CA) was selected through a band-pass filter and shuttered. Fluorescently labeled Mad2 kinetochores were imaged before and after opening the laser for 25 ms. The microscope and shutters were controlled by MetaMorph imaging software (Universal Imaging Corp.). For analysis of Mad2 localization at 23°C, injected cells were imaged from prometaphase through anaphase at 6-min intervals, and a through-focal series was taken after the last chromosome congressed to ensure that Mad2 had been depleted.

For DIC time-lapse imaging, images were obtained with a Hamamatsu C4880 cooled CCD digital camera, using a Nikon Microphot FX-A microscope equipped with a 60×/1.4 NA objective lens (Hoffman *et al.*, 2001). This scope was in a room where the temperature was kept at 23–24°C.

Data Analysis

Kinetochore fluorescence, minus background, and out-of-focus fluorescence, was quantified using MetaMorph imaging software and the primary 12-bit images as previously described (Hoffman *et al.*, 2001; King *et al.*, 2000). Briefly, computer-generated 9 × 9 and 13 × 13 pixel regions were centered over each kinetochore and the total integrated fluorescent counts were obtained for each region. These data were transferred into Microsoft Excel using the MetaMorph Dynamic Data Exchange function. Background fluorescence was calculated by subtracting the fluorescence of the inner square from the fluorescence of the outer square and multiplying to scale for the difference in areas. The integrated fluorescence of the kinetochore was calculated by subtracting the background fluorescence. Two-tailed statistical *t* tests were performed between measurements of kinetochores at 23 and 37°C.

FRAP analysis was performed as described (Howell *et al.*, 2000). In brief, MetaMorph software was used to determine integrated fluorescence intensities at the kinetochore. Graphs of integrated intensity minus background vs. time were plotted in Excel. The first-order rate constant k was derived from the slope of the best-fit line through the graph of ln (recovery) vs. time for photobleached regions. The half-life of fluorescence recovery was calculated by $t_{1/2} = \ln 2/k$.

Interkinetochore distances were calculated as previously described (Waters *et al.*, 1996; Hoffman *et al.*, 2001). CREST antigen was used to label kinetochores in prophase and metaphase cells at 23 and 37°C. Primary 12-bit image stacks were calibrated at the appropriate pixel-to-micrometer ratio using MetaMorph imaging software, and interkinetochore distances were measured using linear pixel regions and recorded into Microsoft Excel spreadsheets (Redmond, WA).

RESULTS

PtK1 Cells Have a Prolonged Metaphase at 23°C

PtK1 cells have been reported to undergo a prolonged mitosis when shifted from 35–37°C to 24–25°C (Rieder, 1981), although their kinetochores acquire normal numbers of kinetochore microtubules (24 ± 5; Cassimeris *et al.*, 1988; McEwen *et al.*, 1997). PtK1 cells that are in prophase with dissipated nucleoli will progress through mitosis when shifted to hypothermic conditions but spend longer in prometaphase and metaphase than cells at 37°C. The time between nuclear envelope breakdown and anaphase onset was 8–12 h for the hypothermic cells, compared with 0.5–1 h at 37°C (Rieder, 1981). Cells that are in interphase at the time of the shift will not enter mitosis until returned to the higher temperature (Rieder and Borisy, 1981).

To further investigate the origins of this mitotic delay, we first wanted to determine the length of the metaphase delay in our PtK1 cell line. Coverslips of PtK1 cells were removed from 37°C and placed in media at room temperature (23–25°C) for 1 h before observation. Then, cells were mounted in Rose chambers and imaged at 23–25°C using either DIC or phase contrast time-lapse microscopy. PtK1 cells in late prometaphase were chosen for observation and imaged until telophase. The total time in metaphase was calculated from the time of congression of the last chromosome to the metaphase plate until the time of anaphase onset. At 23°C, cells spent an average of 101 min in metaphase (N = 12). The total time in metaphase ranged from 55 to 170 min. The cell in Figure 1 completed congression at 00:00 and entered anaphase at 1:08:44. This is in contrast to our PtK1 cells at 37°C, which spent an average of 21 min in metaphase (N = 8), ranging from 8 to 32 min. This period is similar to previous findings that PtK1 cells at 37°C spend an average of 23 min between when the last chromosome begins congression and anaphase onset (Rieder *et al.*, 1994). At the lower temperature, sister kinetochores exhibited poleward and antipoleward oscillations near the spindle equator during the extended metaphase, motility typical of metaphase kinetochores at 37°C but with slightly slower velocities, as previously reported (Wise *et al.*, 1991).

The Metaphase Delay at 23°C Is Due to the Mitotic Checkpoint

The prolonged metaphase exhibited by cells at room temperature could be due to a physical inability to initiate

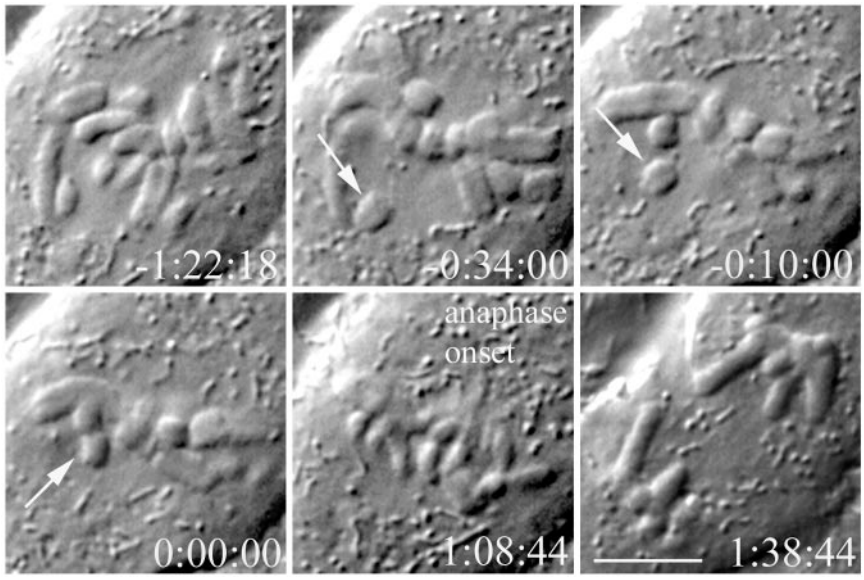

Figure 1. PtK1 cells exhibit a metaphase delay at 23°C. After an extended prometaphase, all chromosomes are aligned at the metaphase plate at 0:00:00. The cell enters anaphase after a lengthy metaphase delay. Time h:min:sec Bar, 5 μm.

anaphase or to activation of the mitotic checkpoint. Injection of a high concentration of anti-Mad2 antibody has been shown to induce premature anaphase in prometaphase PtK1 cells at 37°C (Gorbsky *et al.*, 1998; Waters *et al.*, 1998; Canman *et al.*, 2000). However, the mechanism by which anti-Mad2 antibody induces anaphase is unknown. Recently, a fragment of Mad1 named Mad1F10 (aa 321–556) was shown to induce premature anaphase in Ptk1 cells at 37°C (Canman *et al.*, 2002a,b). This Mad1 fragment contains the Mad1 oligomerization domain and the Mad2 binding domain (Canman *et al.*, 2002a,b) but lacks the kinetochore binding region, because a Mad1 fragment consisting of aa 326–718 is unable to localize to kinetochores (Chung and Chen, 2002). GST-Mad1F10 acts as a dominant negative by inhibiting the ability of Mad2 to inactivate Cdc20/APC in vitro (Canman *et al.*, 2002).

For these experiments, PtK1 cells on a coverslip were removed from 37°C and placed in media at 23°C. After 1 h at 23°C, coverslips were placed in a Rose chamber and late prometaphase cells, often with only a single noncongressed chromosome, were observed by time-lapse phase microscopy. At the beginning of metaphase (T = 00:00), after the last chromosome arrived at the metaphase plate, cells were injected with GST-Mad1F10. There was an interval of several minutes between entry into metaphase and the time of injection, so results for both time from injection to anaphase onset and total time in metaphase are presented. GST-Mad1F10 induced anaphase within 32 ± 6 min (N = 5) after injection. The injection of GST-Mad1F10 into PtK1 cells at 23°C reduced the total time spent in metaphase to 36 ± 4 min. The cell in Figure 2A entered metaphase (00:00) and then was injected with GST-Mad1F10 at 02:20. The cell entered anaphase after spending 36:21 min in metaphase. Control cells at 23°C, injected in metaphase with GST alone spent an average of 74 min total in metaphase (N = 3), and were within the range for uninjected cells at 23°C.

Similar results were seen with anti-Mad2 antibody (N = 10), which induced anaphase onset an average of 20 ± 8 min after injection into PtK1 cells at 23°C. This is similar to the activity of the antibody at 37°C, which induces premature anaphase in prometaphase cells after an average of 11 min (Canman *et al.*, 2000). Anti-Mad2 antibody injected cells at 23°C spent an average of 29 ± 6 min total in metaphase, which is similar to the 21 min in metaphase exhibited by PtK1 cells at 37°C. The cell in Figure 2B entered metaphase at 00:00 and was injected with anti-Mad2 antibody ~6 min later. The cell entered anaphase at 27:28, 21.5 min after antibody injection. This is dramatically shorter than the 73 min total in metaphase exhibited by rabbit IgG control-injected cells (N = 3) at 23°C.

These data suggest that the metaphase delay at 23°C is due to a lag in inactivating the mitotic checkpoint. The ability of both the GST-Mad1F10 and anti-Mad antibodies to abrogate the metaphase delay at 23°C indicates that the room temperature PtK1 cells are capable of entering anaphase soon after formation of the metaphase plate.

Mad2 Is Undetectable at Metaphase Kinetochores at 23°C

Mad2 localization to kinetochores has been shown to be dependent on microtubule attachment rather than the tension generated by biorientation (Waters *et al.*, 1998). Kinetochores of metaphase chromosomes at 23°C acquire normal numbers of kinetochore microtubules (Cassimeris *et al.*, 1988) and therefore are not predicted to exhibit Mad2 localization at kinetochores during the prolonged metaphase. Visualization of Mad2 dynamics in live PtK1 cells at 37°C revealed that anaphase onset occurs 10 min after depletion of Mad2 from the kinetochore of the last congressing chromosome (Howell *et al.*, 2000), suggesting a temporal link between Mad2 depletion from kinetochores and anaphase onset. We decided to investigate Mad2 dynamics in PtK1 cells at 23°C to determine if Mad2 depletion from kinetochores was correlated with anaphase onset.

To visualize Mad2 at kinetochores during metaphase at 23°C, we injected fluorescently labeled Alexa488-XMad2 into prometaphase PtK1 cells that had been at 23°C for 1 h.

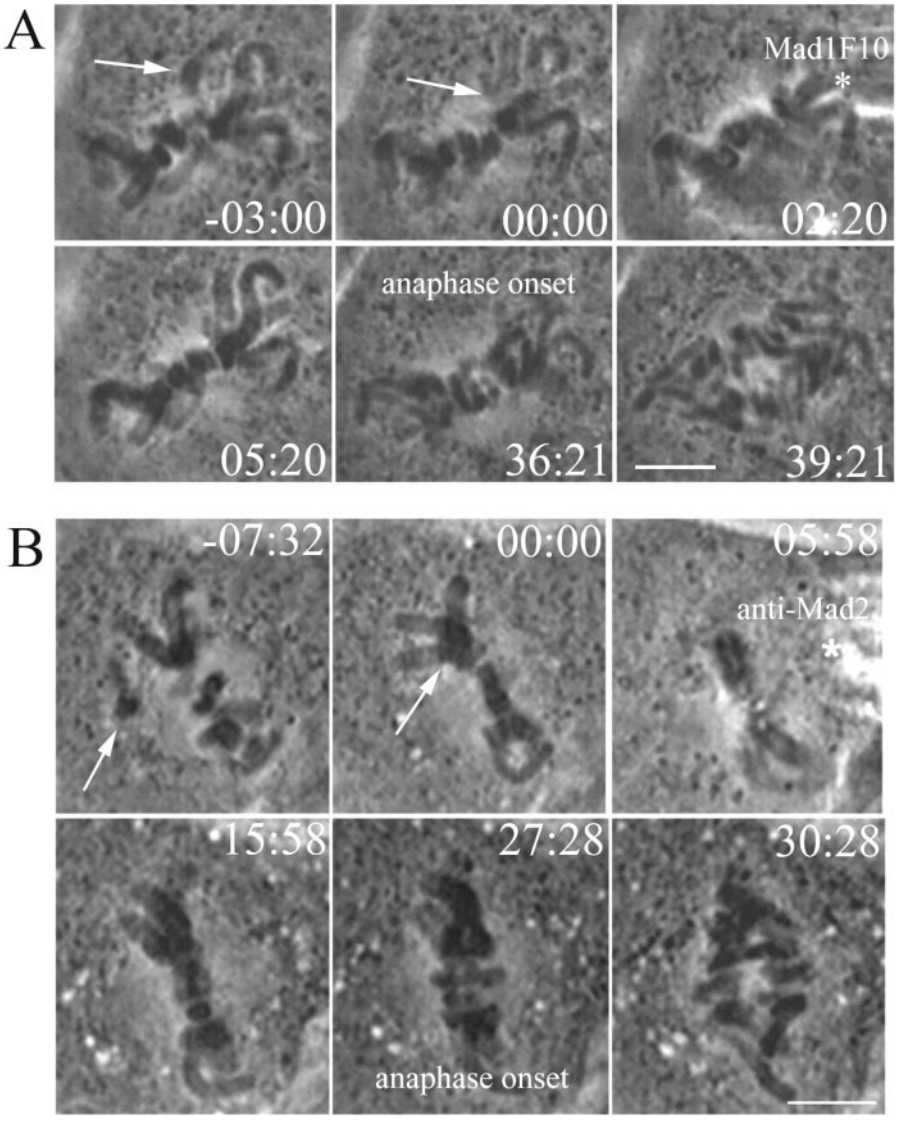

Figure 2. Mad2 is required for the metaphase delay at 23°C. (A) Injection of GST-Mad1F10 eliminates the metaphase delay in PtK1 cells at 23°C. After all chromosomes reached alignment at the metaphase plate (arrow), the cell was injected with GST-Mad1F10 (asterisk). The cell entered anaphase a short time later. Time is shown in minutes:seconds. Bar, 5 μm. (B) Injection of anti-Mad2 antibody eliminates the mitotic delay in PtK1 cells at 23°C. After the last chromosome reached alignment at the metaphase plate (arrow), the cell was injected with anti-Mad2 antibody (asterisk). The cell entered anaphase a short time later. Time is shown in minutes:seconds. Bar, 5 μm.

Injected cells were followed by phase and epifluorescent time-lapse microscopy. Mad2 appeared to localize normally at 23°C, appearing at unattached kinetochores and often at spindle poles proximal to labeled kinetochores, as reported by Howell *et al.* (2000) for cells at 37°C. After chromosome congression to the metaphase plate, Mad2 became undetectable at the newly aligned kinetochore within 6–18 min, a duration similar to its dynamics at 37°C. However, at 23°C Mad2 was lost from the kinetochore of the last congressing chromosome an average of 80 min before anaphase onset (N = 10), whereas at 37°C, anaphase onset occurs an average of 10 min after Mad2 disappears from the last congressing chromosome (Howell *et al.*, 2000).

An example is shown in Figure 3. Mad2 is visible at the kinetochore as the last chromosome reaches the metaphase plate (arrows), and Mad2 is no longer visible at the kinetochore within 7 min of biorientation as viewed by Z-series optical sectioning. After Mad2 is lost from the kinetochore, it persists at the proximal pole (arrowhead), behavior that is also seen in PtK1 cells at 37°C. The cell enters anaphase at 1:13:12, 54 min after Mad2 is no longer visible at kinetochores or spindle poles. This is much longer than the 10 min between loss of Mad2 and anaphase onset at 37°C (Howell *et al.*, 2000).

We also investigated the turnover of Mad2 at kinetochores at 23°C using measurements of Fluorescence Recovery After Photobleaching (FRAP). Prometaphase PtK1 cells at room temperature were injected with Alexa488-XMad2 protein as described above. During time-lapse acquisition, labeled, unattached, or partially attached kinetochores were photobleached using a 25-ms exposure from a focused argon laser, and recovery was monitored for 5 min. The $t_{1/2}$ was calculated using MetaMorph software as previously described (Howell *et al.*, 2000). At 23°C, Alexa488 Mad2 turns over with a $t_{1/2}$ of 36 s (N = 15). Mad2 fluorescence recovery was nearly complete, returning on average to 97% of initial bleached fluorescence. In Figure 4, the kinetochore is

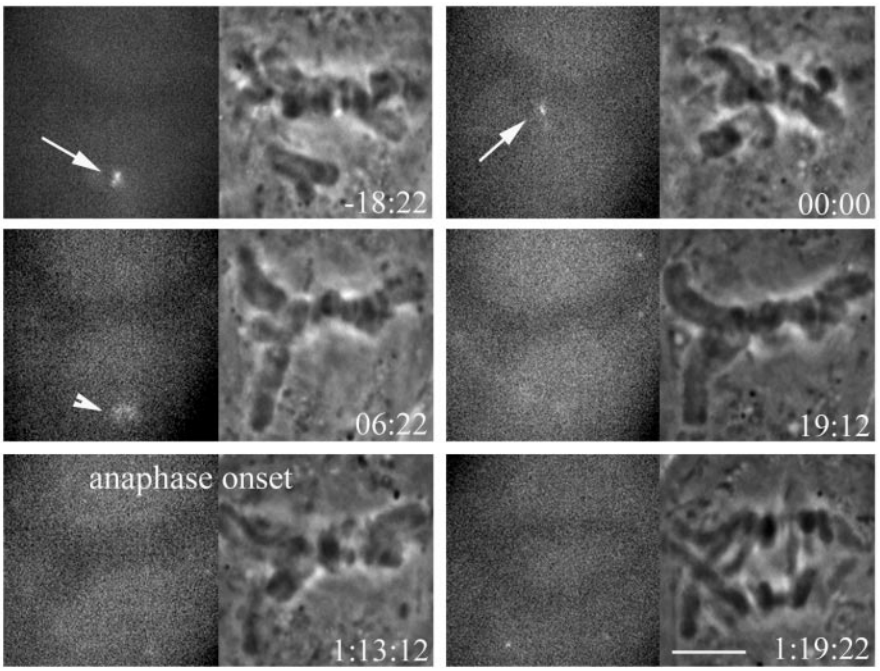

Figure 3. Fluorescent and phase-contrast time lapse images of a living mitotic PtK1 cell at 23°C injected with Alexa-488XMad2. Fluorescent XMad2 localizes to the kinetochore of the unaligned chromosome (arrow), and becomes lost as the chromosome reaches the metaphase plate. Mad2 fluorescence is also briefly visible at the proximal spindle pole (arrowhead). The cell remains in metaphase long after fluorescent Mad2 is no longer visible at the kinetochore or spindle pole. Time is shown in hours:minutes: seconds. Bar, 5 μm.

bleached at 24 s and has reached half-recovery at 1:00, 36 s after bleaching. By 2:10, the kinetochore has recovered to prebleach levels. The $t_{1/2}$ is slightly longer at 23°C than the $t_{1/2}$ of 24 s at 37°C, but this difference is in the wrong direction to explain the 80-min delay between loss of Mad2 and anaphase onset, if checkpoint activity depends on the rate of Mad2 turnover at kinetochores (Fang *et al.*, 1998; Gorbsky *et al.*, 1998; Howell *et al.*, 2000).

Live cell analysis at 23°C reveals that Mad2 exhibits rapid turn over at kinetochores and is depleted from kinetochores soon after chromosome congression. This shows that at 23°C, loss of Mad2 from kinetochores is not sufficient to induce anaphase onset. The metaphase delay at 23°C is not due to detectable Mad2 persisting at attached, aligned kinetochores or spindle poles

Metaphase Kinetochores Are under Reduced Tension at 23°C Compared with 37°C

At metaphase, bioriented chromosomes are under tension because of net pulling forces of opposing microtubules

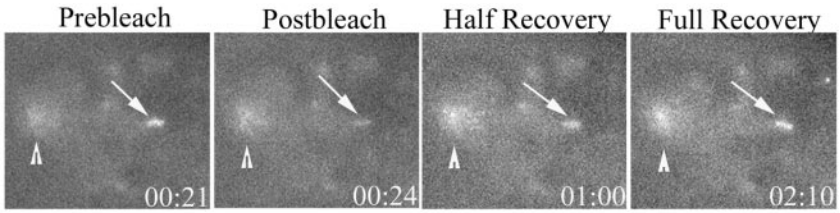

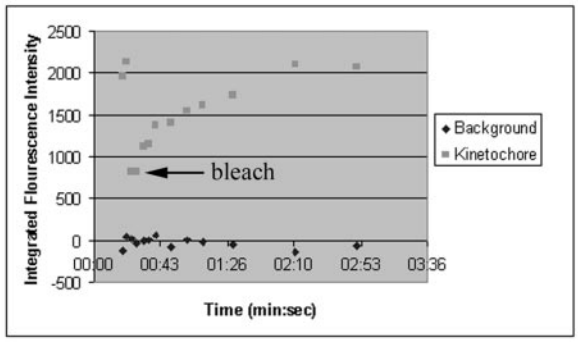

Figure 4. FRAP analysis of Mad2 turnover at kinetochores in PtK1 cells at 23°C. (A) Cells were fluorescently imaged before and after photobleaching of a single kinetochore (arrow). Arrowhead represents Mad2 at the spindle pole. Prebleach, postbleach, and recovery images are shown. Time is in minutes:seconds. (B) Corresponding FRAP graph of Mad2 turnover at the bleached kinetochore. Square represents the kinetochore, while the diamonds are measurements of background fluorescence. Arrow represents time of photobleaching.

Table 1. Interkinetochore distances

	Distances	No. of chromosomes/cells
23°C prophase	1.3 ± 0.19 (1.0–1.8)	35/4
37°C prophase	1.2 ± 0.08 (1.1–1.4)	25/3
23°C metaphase	2.9 ± 0.72 (1.8–4.6)	110/12
37°C metaphase	3.3 ± 0.7 (1.8–4.9)	102/11

Values are means ± SD in μm, with range in parentheses.

(Khodjakov *et al.*, 1996; Waters *et al.*, 1998). To test if tension is affected at 23°C, we measured the stretch of the centromeric chromatin between sister kinetochores. The distance between sister kinetochores reflects the amount of tension, because sister kinetochores are further apart at metaphase than at prophase or in taxol, where there are no pulling forces (Waters *et al.*, 1998).

PtK1 coverslips were permeablized and fixed at 23°C after 1 h at 23°C. Control cells were permeablized and fixed at 37°C. Cells were then processed in parallel for immunofluorescence labeling of kinetochores using CREST serum, which recognizes the core kinetochore proteins CENP-A, -B, and -C (Maney *et al.*, 2000). Immunofluorescence images were collected as Z-series optical sections and analyzed using MetaMorph software. Interkinetochore distance was calculated as previously described (Waters *et al.*, 1996, 1998). As shown in Table 1, the distance between sister kinetochores at prophase, or the rest length, at either 23 or 37°C was similar, 1.3 and 1.2 μm, respectively. At metaphase, when chromosomes are stretched by pulling forces at sister kinetochores, there was a small but statistically significant difference in the average interkinetochore distance between metaphase cells at 23 and 37°C. At 23°C, the distance was 2.9 μm compared with 3.3 μm at 37°C ($p < 0.0005$). Therefore, the average centromere stretch at metaphase (distance at metaphase minus rest length) was 1.6 μm at 23°C and 2.1 μm at 37°C. This indicates that at 23°C metaphase kinetochores are under 24% less tension on average than metaphase kinetochores at 37°C. This difference in tension may be responsible for the prolonged metaphase delay at room temperature.

Quantification of Mad2, 3F3/2, Bub1, and BubR1 at Metaphase Kinetochores

There are many kinetochore components involved in the mitotic checkpoint. Although Mad2 localization at kinetochores has been shown to be dependent on microtubule attachment (Waters *et al.*, 1998), other factors have been shown to be responsive to tension. For example, the 3F3/2 phosphoepitope is dephosphorylated in response to tension (Nicklas *et al.*, 1995), independent of microtubule attachment (Waters *et al.*, 1998). Also, the localization of the kinases Bub1 and BubR1 has been reported to be responsive to loss of tension in HeLa cells (Skoufias *et al.*, 2001; Taylor *et al.*, 2001). Because of the relative decrease in tension found at room temperature metaphase kinetochores, we were interested in determining the levels of these kinetochore components at 23°C.

Table 2. Integrated kinetochore fluorescence intensities at 23 and 37°C

	Intensity		
	23°C	37°C	p
Mad2 unaligned	7737 ± 1967 (14)	8102 ± 2348 (14)	0.659
Mad2 aligned	233 ± 155 (11)	242 ± 77 (19)	0.871
3F3 unaligned	22374 ± 8952 (18)	22836 ± 7589 (17)	0.687
3F3 aligned	5980 ± 3656 (75)	4386 ± 3015 (81)	0.004
BubR1 unaligned	24071 ± 6921 (16)	29205 ± 7038 (19)	0.037
BubR1 aligned	8483 ± 5171 (109)	6242 ± 3664 (101)	0.0003
Bub1 unaligned	16150 ± 9813 (51)	15504 ± 5152 (74)	0.668
Bub1 aligned	4734 ± 2320 (117)	3756 ± 1881 (117)	0.0004

Values are means ± SD, with n in parentheses.

PtK1 cells were fixed at 23°C after 1 h at 23°C, whereas control cells were fixed at 37°C. Immunofluorescence of Mad2, 3F3/2, Bub1, and BubR1 was performed as described in MATERIALS AND METHODS. Z-series optical stacks of images were acquired, and quantification of average integrated fluorescence was performed using Metamorph software (King *et al.*, 2000; Hoffman *et al.*, 2001). Only kinetochores exhibiting fluorescence were measured, without taking into account kinetochores that lacked staining. All metaphase kinetochores exhibit detectable 3F3/2, Bub1, and BubR1 staining, whereas few had detectable Mad2. Therefore the Mad2 measurements are likely to be overestimates of the average. Similar numbers of kinetochores were measured per cell.

Mad2 levels at unaligned and aligned metaphase kinetochores were calculated at 23 and 37°C. Results are shown in Table 2, and normalized fluorescence is shown in Figure 5A. As previously reported (Hoffman *et al.*, 2001), Mad2 levels are very high at unaligned kinetochores and drop dramatically at metaphase kinetochores. There was no appreciable difference in Mad2 levels between unaligned kinetochores at 23 and 37°C or between metaphase kinetochores at 23 and 37°C. The fixed cell analysis is consistent with the similar Mad2 dynamics observed in live cells at 23 and 37°C.

Table 2 also shows the measured 3F3/2 levels at kinetochores. Similar amounts of 3F3/2 were found at unaligned kinetochores at 23 and 37°C. However, the metaphase kinetochores at 23°C had a 37% higher level of 3F3/2 fluorescence than metaphase kinetochores at 37°C. This difference is statistically significant ($p < 0.005$). Normalized values are shown in Figure 5B. Metaphase kinetochores at 37°C had five times less 3F3/2 than at prophase, whereas at 23°C metaphase kinetochores had a less than fourfold reduction in 3F3/2 fluorescence compared with prophase. The higher 3F3/2 fluorescence at 23°C is consistent with the measured decrease in tension at these kinetochores.

Bub1 fluorescence intensities are shown in Table 2. There is no statistical difference in Bub1 levels on unaligned kinetochores at 23°C compared with 37°C. However, Bub1 levels on aligned kinetochores at 23°C were increased 26% >37°C levels. The difference in Bub1 levels at metaphase between the two temperatures was statistically significant ($p < 0.0005$). Normalized values are shown in Figure 5C.

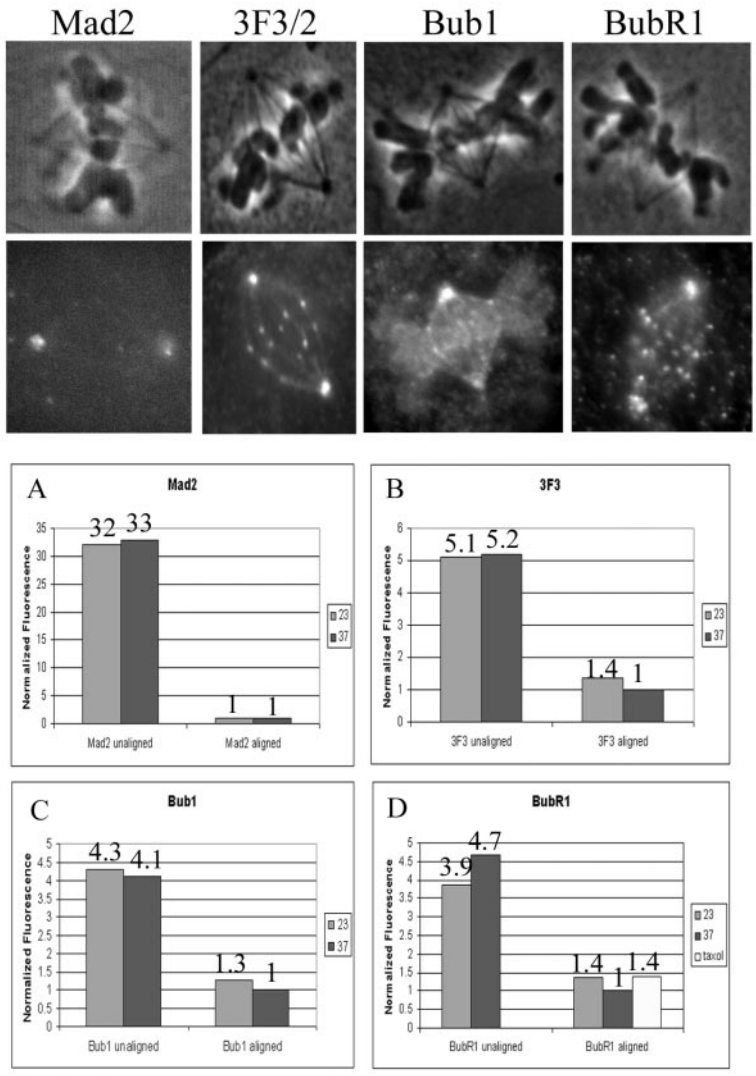

Figure 5. Fluorescent intensities of kinetochores at 23 and 37°C. Top panels show representative fluorescent images of PtK1 cells at 23°C stained with the antibodies indicated. (A–D) Quantitative comparison of relative changes in fluorescence. Values from Table 2 were normalized using the fluorescence at aligned kinetchores at 37°C.

BubR1 fluorescence was also calculated for kinetochores at 23 and 37°C. BubR1 levels were similar on unaligned kinetochores at both temperatures. As shown in Table 2, BubR1 levels were 36% higher at aligned metaphase kinetochores at 23°C than those at 37°C ($p < 0.0005$). Normalized fluorescence is shown in Figure 5D. Metaphase kinetochores at 37°C exhibited a nearly fivefold reduction in BubR1 levels relative to unattached kinetochores, similar to previous observations (Hoffman *et al.*, 2001). In contrast, at 23°C, metaphase kinetochores had only about a threefold reduction in BubR1 levels.

It seems likely that the decrease in tension at 23°C is responsible for the increased BubR1 levels at kinetochores; however, we had previously not seen an increase in BubR1 levels after loss of tension in Ptk1 cells treated with taxol (Hoffman *et al.*, 2001). We repeated measurements of BubR1 levels at metaphase kinetochores in Ptk1 cells at 37°C with and without 10 μM taxol. Treatment of cells with taxol for 45 min caused a complete loss of tension, as interkinetochore distance was reduced to that of prophase cells. BubR1 levels on aligned metaphase kinetochores were increased 38% in taxol-treated cells compared with controls (Figure 5D). This increase in response to taxol is small but statistically significant ($p = 0.0003$). This increase in BubR1 levels after taxol treatment is similar to the increase seen at 23°C, evidence that the elevated BubR1 levels are indeed the result of decreased tension.

This analysis of kinetochore components shows that at 23°C, metaphase levels of 3F3/2, Bub1, and BubR1 fluorescence are elevated compared with 37°C (Table 2 and Figure 5). Although the elevation is subtle, it is statistically significant and correlates with the slight decrease in tension. Initial levels of kinetochore components at unaligned kinetochores are not significantly different at the two temperatures. Presumably, the increase in levels of kinetochore components at metaphase is due to the decrease in tension at the lower temperature. There is no significant difference in Mad2 levels at 23 versus 37°C, consistent with our live cell observations and previous findings that Mad2 levels

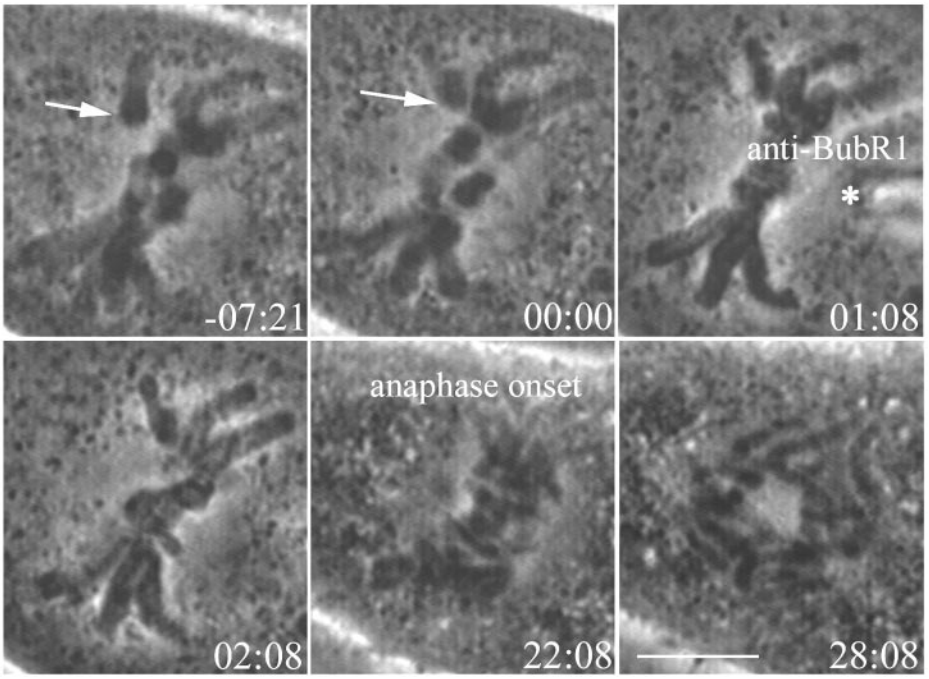

Figure 6. Injection of anti-BubR1 antibody abrogates the metaphase delay in PtK1 cells at 23°C. After the last chromosome reached alignment at the metaphase plate (arrow), the cell was injected with anti-BubR1 antibody (asterisk). The cell entered anaphase a short time later. Time is shown in minutes:seconds. Bar, 5 μm.

are regulated by attachment, not tension (Waters *et al.*, 1998).

Microinjection of BubR1 Antibodies Abrogates the Metaphase Delay

Because we found elevated levels of BubR1 on metaphase kinetochores at 23°C, we were interested in determining if BubR1 was required for the checkpoint-induced delay. To test this we microinjected anti-BubR1 antibody into PtK1 cells. Previous studies have shown that microinjection of BubR1 antibody into HeLa cells prevents mitotic arrest in the presence of nocodazole (Chan *et al.*, 1999).

PtK1 cells that had been at 23°C for 1 h were mounted in modified Rose chambers as described. Prometaphase cells were filmed until the last congressing chromosome arrived at the metaphase plate. Cells were then microinjected with anti-BubR1 antibody, and filming continued until cells had reached telophase. Injected antibodies brightly labeled kinetochores. Injection of anti-BubR1 antibody reduced the time spent in metaphase at 23°C. The average time from injection to anaphase onset was 16 $\pm$ 4 min (N = 5). The total time these cells spent in metaphase was 19 $\pm$ 2 min. This is in contrast to control cells injected with rabbit IgG, which spent an average of 73 min in metaphase (N = 3), within the range for uninjected cells at 23°C. The PtK1 cell at 23°C in Figure 6 aligned all chromosomes at the metaphase plate and was injected (asterisk) with anti-BubR1 at 1:08 min. The cell entered anaphase after spending 22:08 min in metaphase. The ability of the anti-BubR1 antibody to greatly reduce time spent in metaphase at 23°C indicates that BubR1 is required for the checkpoint-dependent delay.

Double Microinjections Suggest That There Is a Single Checkpoint Pathway

Skoufias *et al.* (2001) proposed that Mad2 and BubR1 act in independent checkpoint pathways responding to attachment and tension, respectively. We reasoned that if there were two different inhibitory complexes, inhibiting both Mad2 and BubR1 may induce anaphase more quickly than inactivating only one.

Ptk1 cells at 23°C were injected as described previously. Early metaphase cells were first injected with GST-Mad1F10, then after a few minutes injected with anti-BubR1 antibody. Cells entered anaphase an average of 31 $\pm$ 8 min after the GST-Mad1F10 injection (N = 5), spending an average of 36 $\pm$ 6 min in metaphase. The cell in Figure 7 was injected with GST-Mad1F10 at 4:15 min. Anti-BubR1 antibody was injected soon after, and anaphase onset occurred at 29:50, 25 min, 35 s after the initial injection. This is nearly identical to the results seen with GST-Mad1F10 injection alone (Figure 2A), which induced anaphase after an average of 32 min and is within the range expected for anti-BubR1 single injections. These results suggest that there is a single mitotic checkpoint pathway that depends on both Mad2 and BubR1.

Mad1F10 Abrogates the Checkpoint in HeLa Cells Treated with Low Levels of Vinblastine

The hypothesis that Mad2 and BubR1 function in two separate pathways was based on studies with HeLa cells (Skoufias *et al.*, 2001). As a further test of this hypothesis, we treated HeLa cells with 6.7 nM vinblastine, which has been shown to reduce tension and induce mitotic arrest (Skoufias *et al.*, 2001) and microinjected GST-Mad1F10 as described in MATERIALS AND METHODS (N = 5). Microinjection of Mad1F10 disrupted the mitotic checkpoint, allowing the

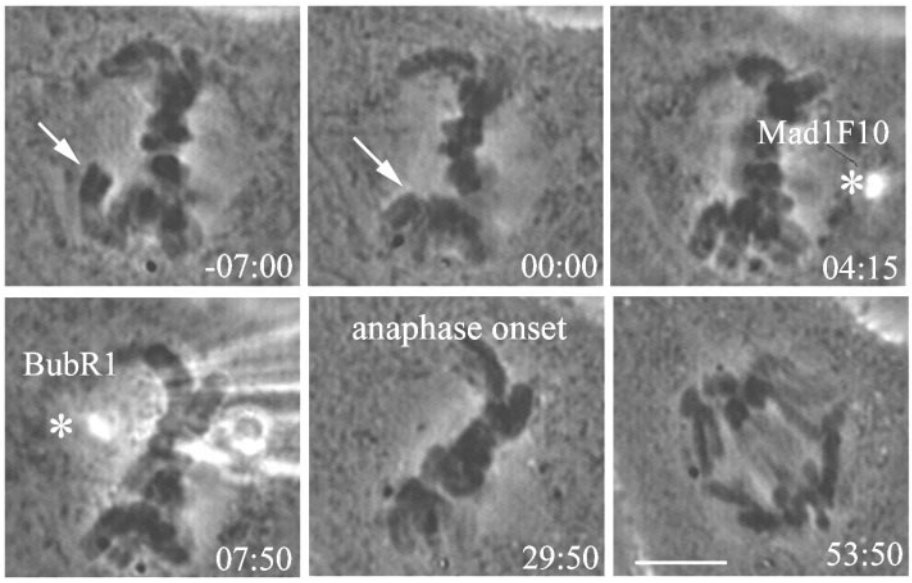

Figure 7. Double injection of GST-Mad1F10 and anti-BubR1 antibody suggests that there is a single mitotic checkpoint pathway. After the PtK1 cell at 23°C reaches metaphase (arrow), it is injected first with GST-Mad1F10 and then with anti-BubR1 antibody (asterisks). The cell enters anaphase at 29:50. Time is shown in min:sec. Bar, 5 μm.

cells to exit mitosis. These cells began blebbing on average 73 ± 12 min after injection, indicative of C phase. C phase occurs when cells exit mitosis in the absence of microtubules; the cell cortex has a defined period of contractility during which cytokinesis can occur if microtubules are allowed to reform (Canman *et al.*, 2000). The blebbing during C phase follows anaphase (Canman *et al.*, 2000), but the separation of chromatids was not visible because of the rounding of HeLa cells during mitosis. The cells continued to blebb for an average of 52 ± 14 min before beginning to respread and reform nucleoli and nuclear envelope without completing cytokinesis. An example is shown in Figure 8. The cell in vinblastine was injected with Mad1F10 (00:00) and began to exhibit contractility at the cortex at 1:41. After extensive blebbing, the cell began to respread at 2:05, and reforming nucleoli are visible at 2:26. In control experiments,

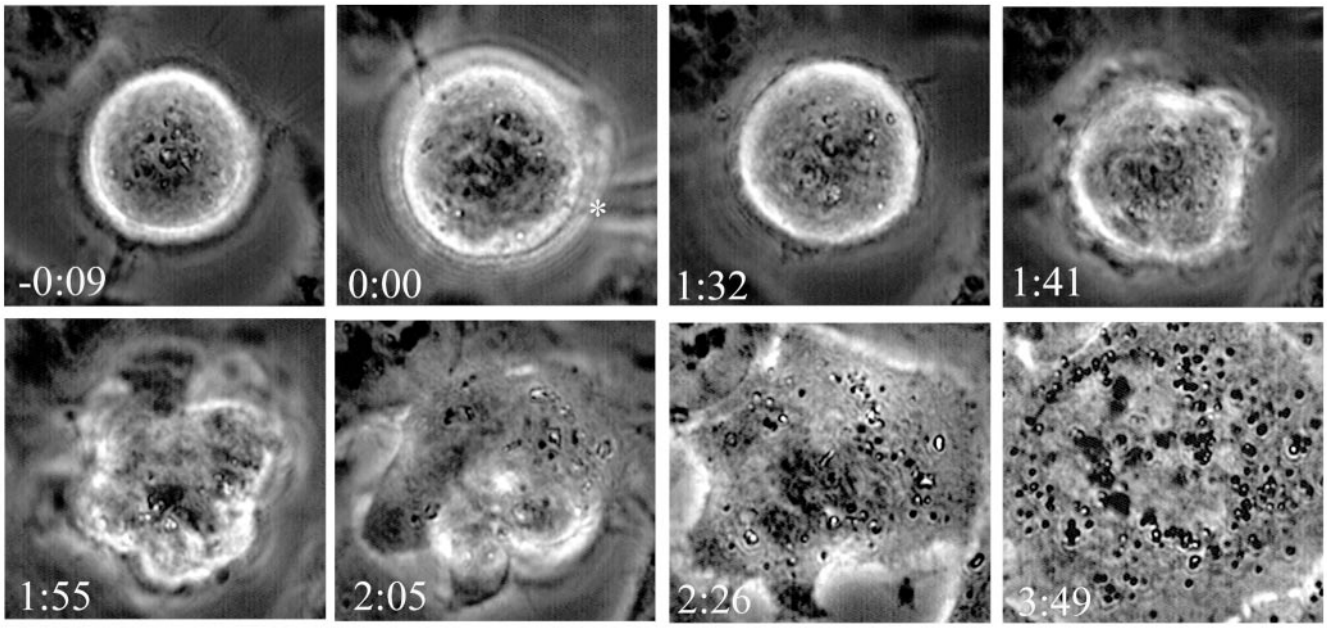

Figure 8. Microinjection of Mad1F10 abrogates the checkpoint in HeLa cells treated with low doses of vinblastine. HeLa cells in 6.7 nM vinblastine were injected with GST-Mad1F10 (asterisk). The cell enters C phase, then respreads and reforms nucleoli, indicating exit from mitosis. Time is shown in h:min.

microinjection of GST alone did not induce C phase or mitotic exit (N = 3), and these control cells remained rounded and mitotic for the duration of filming (>2 h). These experiments demonstrate that perturbation of Mad2 function disrupts the mitotic arrest caused by a loss of tension in HeLa cells.

DISCUSSION

Hypothermic Conditions Result in Decreased Tension and a Checkpoint-mediated Delay in PtK1 Cells

Previously, PtK1 cells were shown to have a prolonged mitosis when cooled from 37 to 23°C (Rieder, 1981). Because these cells have a normal number of kinetochore microtubules (Cassimeris *et al.*, 1988) and chromosomes retain the ability to oscillate at the metaphase plate (Wise *et al.*, 1991), the reason for the mitotic delay was unknown. Here we have shown that kinetochores at 23°C are under less tension on average than those at 37°C. This analysis assumes that the stiffness of the centromeric chromatin does not change with temperature. In support of this assumption, we found that the 3F3/2 labeling at 23°C is higher than at 37°C. Nicklas *et al.* (1995) have shown that loss of 3F3/2 labeling at kinetochores is directly dependent on tension. Whether this decrease in tension is due to reduced microtubule dynamics or a slowing of motor activity at the lower temperature is unclear. It is likely that the decrease in tension is the cause of the prolonged metaphase. Tension is monitored by the checkpoint, as tension from a microneedle on a misattached chromosome leads to anaphase onset (Li and Nicklas, 1995). It is somewhat surprising that the checkpoint is sensitive to a 24% reduction in tension, but this reduction results in a delay, not an arrest. A similar phenomenon was observed in grasshopper spermatocytes where weakly attached chromosomes, which have few kinetochore microtubules and are under reduced tension, delay but do not prevent anaphase onset (Nicklas *et al.*, 2001). In budding yeast, it has been shown that the lack of tension at attached, unreplicated kinetochores produces a mitotic delay but not a block, much as we have described here for Ptk1 cells at 23°C. As we have shown in our studies, the tension dependent delay in yeast is also dependent on Mad2 (Stern and Murray, 2001). The delay in metaphase at 23°C is due to the spindle checkpoint, because once the checkpoint is inactivated by injection of GST-Mad1F10, anti-Mad2 antibody, or anti-BubR1 antibody, the cells enter anaphase.

Although we cannot completely rule out the possibility that the metaphase delay is due to prolonged lifetime or stability of the inhibitory complex bound to Cdc20 at 23°C, we think this is unlikely. This is because microinjection of Mad1F10 substantially shortens the delay. Mad1F10 lacks the kinetochore targeting domain of Mad1 but retains the Mad2 binding domain (Canman *et al.*, 2002a, 2002b; Chung and Chen, 2002), which is nearly identical to the Mad2 binding domain in Cdc20 (Luo *et al.*, 2002). In vitro, Mad2 forms complexes exclusively with either Mad1 or Cdc20 and does not form a Mad1-Mad2-Cdc20 ternary complex (Sironi *et al.*, 2001). Therefore, Mad1F10 likely binds free Mad2 and prevents localization of Mad2 to kinetochores and/or binding of Mad2 to Cdc20 (Canman *et al.*, 2002; Chung and Chen, 2002). Although it is possible that a large excess of Mad1F10 can bind to the Mad2/Cdc20 complex, we feel it is more likely that Mad1F10 disrupts Mad2/Cdc20 by preventing new complex formation, rather than binding directly to Mad2/Cdc20 and accelerating the dissociation rate of this complex. Our data suggest that continual formation of inhibitory complex is necessary for checkpoint activation and the metaphase delay at 23°C.

Localization of Kinetochore Components Is Regulated by Attachment and/or Tension

Previous studies indicated that Mad2 localization to kinetochores is regulated by attachment, not tension (Waters *et al.*, 1998). Our experiments with PtK1 cells at 23°C support this conclusion. Although kinetochores at 23°C have a normal number of microtubules (Cassimeris *et al.*, 1988), there is a slight reduction in tension at all kinetochores. There is no evidence of elevated levels of Mad2 at any kinetochores or poles at 23°C by immunofluorescence of fixed cells. Observation of fluorescently labeled Mad2 in live cells at 23°C showed that Mad2 disappeared from kinetochores and then spindle poles, shortly after chromosome alignment at the metaphase plate, behavior typical of cells at 37°C. Even though no Mad2 was detectable, the cells remained in metaphase for an average of 80 min. It is possible that there is still an undetectable amount of Mad2 at kinetochores that prevents anaphase onset, but using similar techniques and imaging systems, PtK1 cells at 37°C enter metaphase 10 min after Mad2 is no longer detectable. Altered turnover of Mad2 at 23°C is also not able to explain the metaphase delay. Turnover of Mad2 from kinetochores is thought to be important for APC/C inhibition in the cytoplasm (Howell *et al.*, 2000). If Mad2 turnover was increased at 23°C, this would indicate that a greater amount of inhibitory complex may be formed. However, we determined that Mad2 turnover at 23°C was slightly slower than at 37°C.

Bub1 and BubR1 are required for the checkpoint, but unlike Mad2, the localization of these proteins to kinetochores may partly depend on tension. Recent work has shown Bub1 and BubR1 levels, but not Mad2 levels, are partially elevated at HeLa cell kinetochores in response to a decrease in tension caused by low levels of vinblastine or noscapine (Skoufias *et al.*, 2001; Zhou *et al.*, 2002). A similar result is found in our PtK1 cells where tension is reduced by cooling to 23°C. The decrease in tension results in partially elevated levels of Bub1 and BubR1 but not Mad2 on metaphase kinetochores. Similar increases in BubR1 levels are seen after treatment of Ptk1 cells with taxol. After loss of tension, Bub1 and BubR1 levels do not increase to prometaphase levels; therefore, microtubule attachment does play a major role in kinetochore localization of these proteins (Hoffman *et al.*, 2001; Skoufias *et al.*, 2001; Zhou *et al.*, 2002). Bub1 levels at kinetochores in HeLa cells are regulated by both attachment and tension, because microtubule attachment to one sister kinetochore causes a decrease in Bub1 only on the attached sister, and lack of tension caused by taxol treatment of metaphase cells increases Bub1 levels at both attached sister kinetochores (Taylor *et al.*, 2001).

We also found an increase in the phosphorylation recognized by the 3F3/2 antibody in response to decreased tension. Injection of high levels of 3F3/2 antibody has been shown to delay anaphase onset; the epitope remains at kinetochores throughout the prolonged metaphase in injected

cells but disappears by anaphase onset (Campbell and Gorbsky, 1995). The elevated levels of the 3F3/2 epitope during the delay at 23°C reflect the kinetochore's phosphorylated state that suggests that the checkpoint is active. The 3F3/2 epitope has been shown to be depleted in response to tension, reflecting a biochemical change in the kinetochore in response to mechanical forces (Nicklas *et al.*, 1995).

Small Changes at All Kinetochores Can Have an Additive Effect

Even although metaphase 3F3/2, Bub1, and BubR1 levels at 23°C are only 26–37% higher than at 37°C, the levels of these kinetochore components may be sufficient to keep APC/C inactive. A small elevation of protein levels at all 22 Ptk1 kinetochores could have the same effect as a large amount on a single, unattached kinetochore. For example, consider the normalized amounts of BubR1 at kinetochores in Figure 5D. For a metaphase cell at 37°C, the amount of BubR1 at kinetochores would be 1 × 22 kinetochores, or 22 total. For a cell at 37°C with a single unattached kinetochore, BubR1 levels would be 1 × 21 attached kintochores + 4.7 at the unattached kinetochore, or 25.7 total. For a metaphase cell at 23°C, the level of BubR1 is 1.4 × 22 kinetochores, or 30.8. Therefore, the total amount of BubR1 at kinetochores at metaphase at 23°C is greater than in a cell with a single unattached kinetochore. This analysis indicates that small changes at all kinetochores can have a significant additive effect. Not only can a single, unattached kinetochore delay anaphase onset, but attached kinetochores under reduced tension can combine to produce a "wait anaphase" signal. The elimination of the metaphase delay after injection of anti-BubR1 antibodies suggests that this is the case for Ptk1 cells at 23°C.

Two Independent Mitotic Checkpoints or Two Branches of a Single Pathway?

The target of the mitotic checkpoint is the APC/C activator Cdc20. Mad2 has been shown to form a ternary complex with Cdc20 and APC/C, which is inactive (Fang *et al.*, 1998). This led to a model for checkpoint activation in which unattached kinetochores acted to catalyze the formation of the Mad20-Cdc20 complex (Howell *et al.*, 2000).

However, recent work has shown that APC/C regulation is much more complex, and Mad2 is unlikely to be the sole inhibitor. The identification of the MCC and BubR1 as additional APC/C inhibitors complicates our understanding of the checkpoint pathway (Fang, 2002; Skoufias *et al.*, 2001; Tang *et al.*, 2001). Do Mad2 and BubR1 act in independent, parallel pathways? Or do Mad2 and BubR1 function as two branches of the same pathway? We propose that Mad2 and BubR1 act cooperatively in a single pathway to prevent premature anaphase onset. Inactivation of either Mad2 or BubR1 by microinjection of inhibitors shows that the activity of both proteins is required for the metaphase delay at 23°C. Mad2 may function at kinetochores to sense attachment to microtubules, whereas BubR1 monitors tension at the kinetochore. Our analysis of kinetochore component localization in response to a decrease in tension caused by lower temperature supports this model. Even though Mad2 levels are not elevated at kinetochores during the metaphase delay, Mad2 is still required for the checkpoint. It may be that there is a small but undetectable amount of Mad2 at all kinetochores that participate with elevated BubR1 to maintain the checkpoint. Alternatively, the elevated BubR1 at kinetochores may bind Cdc20 and prime Cdc20 for binding to free Mad2. In support of this idea, BubR1 enhances the ability of Mad2 to inhibit Cdc20 activation of APC in vitro (Fang, 2002). Our data also agree with the findings of Chung and Chen (2002) that free Mad2 is required for maintenance of the checkpoint.

The checkpoint response to loss of tension in HeLa cells caused by 6.7 nM vinblastine was reported to be Mad2 independent (Skoufias *et al.*, 2001). However, our data suggest that the two pathways do not act independently of one another, because injection of either GST-Mad1F10 or anti-BubR1 antibodies induces anaphase onset at 23°C with the same timing as injection of both. Also, injection of anti-Mad2 antibody is able to bypass the checkpoint induced by taxol in PtK1 cells at 37°C, which induces the loss of tension without much elevation of kinetochore Mad2 (Waters *et al.*, 1998). Skoufias *et al.* (2001) were not able to induce anaphase in vinblastine arrested cells with the anti-Mad2 antibody. We suspect that the Mad2 antibody from our lab used in their experiments was not fully active. We have found that the antibody loses activity with time, and anti-Mad2 antibody, which can induce premature anaphase in untreated prometaphase cells, is not always competent to induce anaphase in nocodazole-arrested cells. To resolve this issue, we have performed the vinblastine experiments in HeLa cells and found that inhibition of Mad2 by Mad1F10 microinjection does abrogate the checkpoint in response to loss of tension. Therefore, to our knowledge, there is no mitotic checkpoint that does not require Mad2. Our data suggest that Mad2 is essential for a mitotic block in response to either lack of microtubule attachment or loss of tension.

ACKNOWLEDGMENTS

We thank Bonnie Howell for technical assistance and critical reading of the manuscript and G. Fang for generously providing anti-BubR1 antibody for microinjection and all members of the Salmon laboratory and the SPIRE program for assistance and suppport. K.S. is currently a fellow in the Seeding Postdoctoral Innovators in Research and Education (SPIRE) program supported by the Minority Opportunities in Research Division of National Institute of General Medical Sciences grant GM000678. E.D.S. is supported by National Institutes of Health grant GM24364.

REFERENCES

Amon, A. (1999). The spindle checkpoint. Curr. Opin. Genet. Dev. *9*, 69–75.

Campbell, M.S., Daum, J.R., Gersch, M.S., Nicklas, R.B., and Gorbsky, G.J. (2000). Kinetochore "memory" of spindle checkpoint signaling in lysed mitotic cells. Cell Motil. Cytoskelet. *46*, 146–156.

Campbell, M.S., and Gorbsky, G.J. (1995). Microinjection of mitotic cells with the 3F3/2 anti-phosphoepitope antibody delays the onset of anaphase. J. Cell Biol. *129*, 1195–1204.

Canman, J., Salmon, E., and Fang, G. (2002a). Inducing precocious anaphase in cultured mammalian cells. Cell Motil. Cytoskelet. *52*, 61–65.

Canman, J.C., Hoffman, D.B., and Salmon, E.D. (2000). The role of pre- and post-anaphase microtubules in the cytokinesis phase of the cell cycle. Curr. Biol. *10*, 611–614.

Canman, J.C., Sharma, N., Straight, A., Shannon, K.B., Fang, G., and Salmon, E.D. (2002b). The reduced levels of kinetochore and centromere-binding proteins normally seen in anaphase depend on microtubules. J. Cell Sci. (in press).

Cassimeris, L., Inoue, S., and Salmon, E.D. (1988). Microtubule dynamics in the chromosomal spindle fiber: analysis by fluorescence and high-resolution polarization microscopy. Cell Motil. Cytoskelet. *10*, 185–196.

Chan, G.K., Jablonski, S.A., Sudakin, V., Hittle, J.C., and Yen, T.J. (1999). Human BUBR1 is a mitotic checkpoint kinase that monitors CENP-E functions at kinetochores and binds the cyclosome/APC. J. Cell Biol. *146*, 941–954.

Chan, G.K., Schaar, B.T., and Yen, T.J. (1998). Characterization of the kinetochore binding domain of CENP-E reveals interactions with the kinetochore proteins CENP-F and hBUBR1. J. Cell Biol. *143*, 49–63.

Chen, R.H., Shevchenko, A., Mann, M., and Murray, A.W. (1998). Spindle checkpoint protein Xmad1 recruits Xmad2 to unattached kinetochores. J. Cell Biol. *143*, 283–295.

Chen, R.H., Waters, J.C., Salmon, E.D., and Murray, A.W. (1996). Association of spindle assembly checkpoint component XMAD2 with unattached kinetochores. Science *274*, 242–6.

Chung, E., and Chen, R.-H. (2002). The spindle checkpoint requires Mad1-bound and Mad1-free Mad2. Mol. Biol. Cell *13*, 1501–1511.

Fang, G. (2002). The checkpoint protein BubR1 acts synergistically with Mad2 to inhibit the anaphase-promoting complex. Mol. Biol. Cell *13*, 000–000.

Fang, G., Yu, H., and Kirschner, M.W. (1998). The checkpoint protein MAD2 and the mitotic regulator CDC20 form a ternary complex with the anaphase-promoting complex to control anaphase initiation. Genes Dev. *12*, 1871–1883.

Gorbsky, G.J., Chen, R.H., and Murray, A.W. (1998). Microinjection of antibody to Mad2 protein into mammalian cells in mitosis induces premature anaphase. J. Cell Biol. *141*, 1193–1205.

Gorbsky, G.J., and Ricketts, W.A. (1993). Differential expression of a phosphoepitope at the kinetochores of moving chromosomes. J. Cell Biol. *122*, 1311–1321.

Hoffman, D.B., Pearson, C.G., Yen, T.J., Howell, B.J., and Salmon, E.D. (2001). Microtubule-dependent changes in assembly of microtubule motor proteins and mitotic spindle checkpoint proteins at ptk1 kinetochores. Mol. Biol. Cell *12*, 1995–2009.

Howell, B.J., Hoffman, D.B., Fang, G., Murray, A.W., and Salmon, E.D. (2000). Visualization of Mad2 dynamics at kinetochores, along spindle fibers, and at spindle poles in living cells. J. Cell Biol. *150*, 1233–1250.

Hoyt, M.A., Totis, L., and Roberts, B.T. (1991). *S. cerevisiae* genes required for cell cycle arrest in response to loss of microtubule function. Cell *66*, 507–517.

Khodjakov, A., Cole, R.W., Bajer, A.S., and Rieder, C.L. (1996). The force for poleward chromosome motion in Hemanthus cells acts along the length of the chromosome during metaphase but only at the kinetochore during anaphase. J. Cell Biol. *132*, 1093–1104.

King, J.M., Hays, T.S., and Nicklas, R.B. (2000). Dynein is a transient kinetochore component whose binding is regulated by microtubule attachment, not tension. J. Cell Biol. *151*, 739–748.

King, R.W., Deshaies, R.J., Peters, J.M., and Kirschner, M.W. (1996). How proteolysis drives the cell cycle. Science *274*, 1652–1659.

Li, R., and Murray, A.W. (1991). Feedback control of mitosis in budding yeast. Cell *66*, 519–531.

Li, X., and Nicklas, R.B. (1995). Mitotic forces control a cell-cycle checkpoint. Nature *373*, 630–632.

Li, Y., and Benezra, R. (1996). Identification of a human mitotic checkpoint gene: hsMAD2. Science *274*, 246–248.

Li, Y., Gorbea, C., Mahaffey, D., Rechsteiner, M., and Benezra, R. (1997). MAD2 associates with the cyclosome/anaphase-promoting complex and inhibits its activity. Proc. Natl. Acad. Sci. USA *94*, 12431–12436.

Luo, X., Tang, Z., Rizo, J., and Yu, H. (2002). The Mad2 spindle checkpoint protein undergoes similar major conformational changes upon binding to either Mad1 or Cdc20. Mol. Cell *9*, 59–71.

Maddox, P.S., Bloom, K.S., and Salmon, E.D. (2000). The polarity and dynamics of microtubule assembly in the budding yeast *Saccharomyces cerevisiae*. Nat. Cell Biol. *2*, 36–41.

Maney, T., Ginkel, L.M., Hunter, A.W., and Wordeman, L. (2000). The kinetochore of higher eucaryotes: a molecular view. Int. Rev. Cytol. *194*, 67–131.

McEwen, B.F., Heagle, A.B., Cassels, G.O., Buttle, K.F., and Rieder, C.L. (1997). Kinetochore fiber maturation in PtK1 cells and its implications for the mechanisms of chromosome congression and anaphase onset. J. Cell Biol. *137*, 1567–1580.

Nicklas, R.B., Ward, S.C., and Gorbsky, G.J. (1995). Kinetochore chemistry is sensitive to tension and may link mitotic forces to a cell cycle checkpoint. J. Cell Biol. *130*, 929–939.

Nicklas, R.B., Waters, J.C., Salmon, E.D., and Ward, S.C. (2001). Checkpoint signals in grasshopper meiosis are sensitive to microtubule attachment, but tension is still essential. J. Cell Sci. *114*, 4173–4183.

Rieder, C.L. (1981). Effect of hypothermia (20–25 degrees C) on mitosis in PtK1 cells. Cell Biol. Int. Rep. *5*, 563–573.

Rieder, C.L., and Borisy, G.G. (1981). The attachment of kinetochores to the pro-metaphase spindle in PtK1 cells. Recovery from low temperature treatment. Chromosoma *82*, 693–716.

Rieder, C.L., Cole, R.W., Khodjakov, A., and Sluder, G. (1995). The checkpoint delaying anaphase in response to chromosome monoorientation is mediated by an inhibitory signal produced by unattached kinetochores. J. Cell Biol. *130*, 941–948.

Rieder, C.L., and Hard, R. (1990). Newt lung epithelial cells: cultivation, use, and advantages for biomedical research. Int. Rev. Cytol. *122*, 153–220.

Rieder, C.L., Schultz, A., Cole, R., and Sluder, G. (1994). Anaphase onset in vertebrate somatic cells is controlled by a checkpoint that monitors sister kinetochore attachment to the spindle. J. Cell Biol. *127*, 1301–1310.

Salmon, E.D., Inoue, T., Desai, A., and Murray, A.W. (1994). High resolution multimode digital imaging system for mitosis studies in vivo and in vitro. Biol. Bull. *187*, 231–232.

Sharp-Baker, H., and Chen, R.H. (2001). Spindle checkpoint protein bub1 is required for kinetochore localization of mad1, mad2, bub3, and cenp-e, independently of its kinase activity. J. Cell Biol. *153*, 1239–1250.

Sironi, L., Melixetian, M., Faretta, M., Prosperini, E., Helin, K., and Musacchio, A. (2001). Mad2 binding to Mad1 and Cdc20, rather than oligomerization, is required for the spindle checkpoint. EMBO J. *20*, 6371–6382.

Skoufias, D.A., Andreassen, P.R., Lacroix, F.B., Wilson, L., and Margolis, R.L. (2001). Mammalian mad2 and bub1/bubR1 recognize distinct spindle-attachment and kinetochore-tension checkpoints. Proc. Natl. Acad. Sci. USA *98*, 4492–4497.

Stern, B.M., and Murray, A.W. (2001). Lack of tension at kinetochores activates the spindle checkpoint in budding yeast. Curr. Biol. *11*, 1462–1467.

Sudakin, V., Chan, G.K., and Yen, T.J. (2001). Checkpoint inhibition of the APC/C in HeLa cells is mediated by a complex of BUBR1, BUB3, CDC20, and MAD2. J. Cell Biol. *154*, 925–936.

Tang, Z., Bharadwaj, R., Li, B., and Yu, H. (2001). Mad2-Independent inhibition of APCCdc20 by the mitotic checkpoint protein BubR1. Dev. Cell *1*, 227–237.

Taylor, S.S., Ha, E., and McKeon, F. (1998). The human homologue of Bub3 is required for kinetochore localization of Bub1 and a Mad3/Bub1-related protein kinase. J. Cell Biol. *142*, 1–11.

Taylor, S.S., Hussein, D., Wang, Y., Elderkin, S., and Morrow, C.J. (2001). Kinetochore localization and phosphorylation of the mitotic checkpoint components Bub1 and BubR1 are differentially regulated by spindle events in human cells. J. Cell Sci. *114*, 4385–4395.

Taylor, S.S., and McKeon, F. (1997). Kinetochore localization of murine Bub1 is required for normal mitotic timing and checkpoint response to spindle damage. Cell *89*, 727–735.

Waters, J.C., Chen, R.H., Murray, A.W., and Salmon, E.D. (1998). Localization of Mad2 to kinetochores depends on microtubule attachment, not tension. J. Cell Biol. *141*, 1181–1191.

Waters, J.C., Skibbens, R.V., and Salmon, E.D. (1996). Oscillating mitotic newt lung cell kinetochores are, on average, under tension and rarely push. J. Cell Sci. *109*, 2823–2831.

Wise, D., Cassimeris, L., Rieder, C.L., Wadsworth, P., and Salmon, E.D. (1991). Chromosome fiber dynamics and congression oscillations in metaphase PtK2 cells at 23 degrees C. Cell Motil. Cytoskelet. *18*, 131–142.

Zachariae, W., and Nasmyth, K. (1999). Whose end is destruction: cell division and the anaphase-promoting complex. Genes Dev. *13*, 2039–2058.

Zhou, J., Panda, D., Landen, J.W., Wilson, L., and Joshi, H.C. (2002). Minor alteration of microtubule dynamics causes loss of tension across kinetochore pairs and activates the spindle checkpoint. J. Biol. Chem. *277*, 17200–17208.